

Real-time implementation of an enhanced proportional-integral-derivative controller based on sparrow search algorithm for micro-robotics system

Ehab Saif Ghith¹, Farid Abdel Aziz Tolba²

¹Department of Mechatronics, Faculty of Engineering, Ain shams University, Cairo, Egypt

²Faculty of Engineering, Ain shams University, Cairo, Egypt

Article Info

Article history:

Received Aug 12, 2021

Revised Jun 30, 2022

Accepted Jul 29, 2022

Keywords:

Grey wolf optimization
Micro-particles robotics
Minimally invasive surgery
PID Controller
Sparrow search algorithm

ABSTRACT

This paper presents a new approach to control the position of the micro-robotics system with a proportional-integral-derivative (PID) controller. By using sparrow search algorithm (SSA), the optimal PID controller indicators were obtained by applying a new objective function namely, integral square time multiplied square error (ISTES). The efficiency of the proposed SSA-based controller was verified by comparisons made with grey wolf optimization (GWO) algorithm-based controllers in terms of time. Each control technique will be applied to the identified model using MATLAB Simulink and the experimental test facility was conducted using LabVIEW software. The simulation and experimental results show that the performance of SSA-PID controller based on ISTES cost function achieves the best performance among various techniques. Moreover, the SSA technique had the highest performance compared to GWO technique based on rising and setting time and many other performance measurements. Thus, it is recommended to apply SSA for tuning the parameters of PID as it can enhance its performance in micro-robotic systems. It was found that the amount of error is reduced by 50% using SSA than other former experiments.

This is an open access article under the [CC BY-SA](#) license.



Corresponding Author:

Ehab Seif Ghith

Department of Mechatronics, Ain shams University

Cairo, Egypt

Email: Drehabghith1978@gmail.com

1. INTRODUCTION

Minimally invasive surgery (MIS) emphasizes declining the trauma of surgical patients [1]. Also, it makes the clinicians deep-seated every site in the body of the human. Besides, the patient may devote a small-time amount in hospitals, and such may protect a worthy amount of money. One of the likely current surgeries' kinds utilized or implemented today is surgery as laparoscopic. They inserted instruments into the body of humans are through some incisions being small, and the operation is done according to images that are reserved through a camera that is closely attached to the instrument. Figure 1 shows the variance for the two methods of surgery.

The robots usages of MIS are of an advantage to medicine through invasiveness minimizing of MIS. Also, it facilitates the previous treatment of inoperable patients. Such systems as robotic may be implemented to accurately guide the needles to the site as specified in the body of the human. It is associated with the organs as natural in the body of humans according to veins, arteries, and the gastrointestinal tract. They utilize them to aim target as specific needed for treatment, diagnosis, and drug delivery. If the robot came to of smaller size,

the depth of penetration may be elevated inside the body of the human. Such will cause efficient medicine travel pathways to be smaller to achieve their goal.

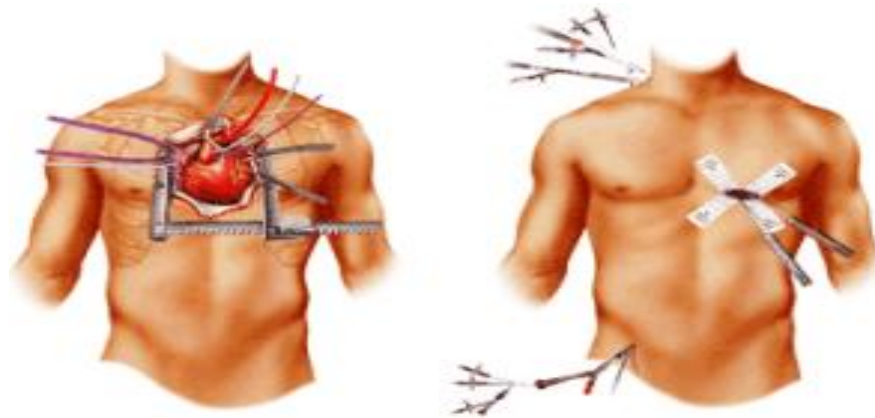


Figure 1. The left image illustrates the traditional open-heart surgery, while the right image manifests the (MIS) heart surgery done using laparoscopic instruments [1]

Keuning *et al.* [2] constructed a controlling system for the spherical site of the paramagnetic micro-particles with 100 μm diameters as average. The system arrived at the control position with a settling error of a maximum of 8.4 μm on a step response experiment with the hollow coil. Extra over, Farag *et al.* [3] implemented the same experiment with a solid coil and attained a maximum settling time equal to 8 μm according to an auto-tuned control system. In our suggested study, the same experiment was done in [3] It may be noticed that the maximum settling error attained is 4 μm . It may be noticed that the amount of error is reduced by 50% than other previous experiments through the Sparrow search algorithm.

For meeting such control goals, the suitable design of a controller is of a vital role. Despite developments in control methods, the controller as proportional-integral-derivative (PID) is still utilized widely in the industry because of its recognized benefits i.e., as not hard to understand because of its just 3 parameters being tunable, the structure being simple, and implementation ease [4]–[8]. Nevertheless, the proper PID tuning as controller gains to achieve optimum performance is quite not easy. Over time, numerous heuristics approaches of design have been suggested. Ziegler and Nichols are among them, some of the most popular customary PID control methods. Generally, it is not easy to get the greatest-tuned gain for achieving the greatest performance through Ziegler and Nichols approach. Likewise, the method of tuning according to the customary method needed extra calculations mathematically that render the system extra complex [9], [10]. To avoid the mentioned problem, recent artificial intelligence-based optimization and tuning methods are favored for controller parameters optimization.

To support meta-heuristic algorithms, optimization techniques are now being used in different engineering fields. The reason of which is that these techniques are very flexible, easy to implement, and do not require gradient information. There are two main categories of meta-heuristics techniques which include population-based algorithms and single-based algorithms. On every run, a single-based optimization algorithm generates a single optimal solution which is also known as trajectory algorithms. Another category is the population-based optimization algorithm which involves the generation of a series of multiple solutions with redundancy. These solutions are further divided into five main categories including physics-based, chemical-based, evolutionary-based, human-based, and swarm intelligence-based algorithms of optimization [11]–[17], [18]–[24].

The current study involves an optimization algorithm called the Sparrow search algorithm (SSA) which has been developed quite recently. SSA has been used by micro-robotic systems to tune the PID controller which is essential to reduce the robustness of integral square time multiplied error square (ISTES). Among the optimization algorithms, SSA is preferred because it is efficient in the frequency and time domain. In this paper, section 2 is about the description of the system and different PID controller types, section 3 is about the details of optimization techniques, section 4 involves the results of simulation and experiment, while sections 5 and 6 include the discussion, conclusion, and future work regarding SSA. These data are collected based on the experimental setup, in which some of experimental results were reported and published in Ref. [3], and this work study is an extension of this work with advanced optimization techniques.

2. RESEARCH METHOD

2.1. Mathematical model

The particle is constructed of a paramagnetic material, and it needs Fe_2O_3 in lactic acid. Such particle is of $100\mu\text{m}$ diameters. The velocity of particles is associated with 2 chief factors. Such factor(s) is the viscous drag force and the force as magnetic applied for micro-particles based on the need field as magnetic through coils. If acceleration arrives at 0, velocity as a maximum is attained, thus, the force as magnetic will be equivalent to the drag viscous force. The magnetic force may be designated,

$$F = \nabla \alpha_p V_p B^2 \quad (1)$$

Since V_p is designated as particles volumes, whereas B is recognized as the magnetic density of flux. B associated with the time and distance, α_p , and V_p are constants. The previous volume of the formula may be substituted to get the force formula as shown in (2),

$$F = \frac{4}{3} \pi \alpha_p r_p^3 \nabla B^2 \quad (2)$$

Since r_p is recognized as the micro radius of particles, whereas the force of drag is signified through as shown in (3),

$$F_d = -6\pi\eta r_p v \quad (3)$$

Since η is viscosity, in which v is designated as micro-particles velocity, and according to 2nd law of Newton motion,

$$\begin{aligned} \Sigma F &= m_p a_p \\ \frac{4}{3} \pi \alpha_p r_p^3 \nabla B^2 - 6\pi\eta r_p v &= m_p a_p \\ v &= \frac{\frac{4}{3} \pi \alpha_p r_p^3 \nabla B^2 - m_p a_p}{6\pi\eta r_p} \end{aligned} \quad (4)$$

Using (4), the maximum velocity takes place if the acceleration of the particle is equal to zero. The velocity as a maximum is designated utilizing (5),

$$v_m = \frac{2}{9} \frac{\alpha_p r_p^2}{\eta} \nabla B^2 \quad (5)$$

Lastly, the particles are regarded as spheres being perfect. It is stimulated utilizing force as magnetic designated through F_m . A force as drag F_d which associated with the particles' speed in respect to the liquid. If the liquid is stable the drag is then associated with the speed of the particle in respect to the world is fixed. The system of continuous-time model is designated through,

$$m\ddot{x} + C_d * \dot{x} = F_m \quad (6)$$

Since C_d the drag is designated continuously through drag Stokes of Reynolds being low, m is the particle mass and \dot{x} is the velocity, and \ddot{x} is the acceleration. The micro-particle transfer role may be signified utilizing (7),

$$\frac{X(s)}{F_m(s)} = \frac{1}{ms^2 + C_d * s} \quad (7)$$

2.2. PID controller

One of the chief controller kinds which are needed in the practice of industry is the proportional-integral-derivative as idyllic (ideal-PID) [4]. Such controller develops the error of state as steady and transient. The PID as ideal loses the higher enactment in the case of the disturbances. Such controllers are recognized as customary ones. Figure 2(a) shows the chief ideal PID controller block diagram. The transfer ideal-PID role is signified utilizing (8),

$$C(s) = \frac{Y(s)}{E(s)} = K_p + \frac{K_i}{s} + K_d s \quad (8)$$

Since the proportional, integral, derivative is designated in the previous formulation is signified utilizing the K_p , K_i , and K_d correspondingly. The general intelligent controller PID structure is illustrated in Figure 2(b). The chief PID controller components are the role of fitness, methods of optimization, sensor, and process.

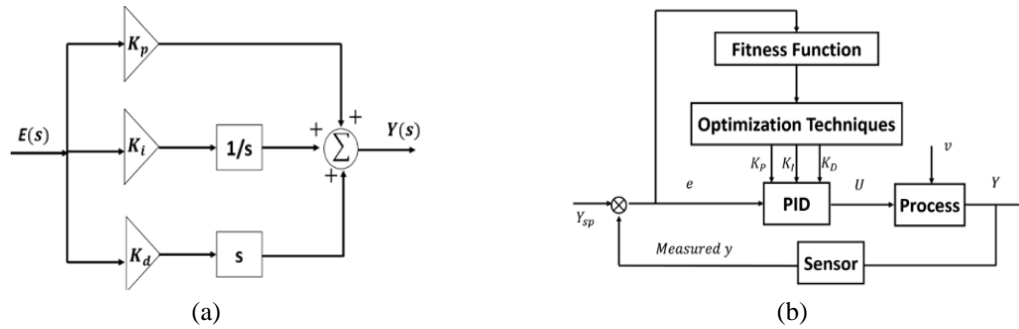


Figure 2. Block diagrams of PID controller for, (a) ideal PID controller and (b) tuning parameters of PID controller

2.3. Fitness function

To design any type of controller there must exist many optimum control parameters. These parameters are estimated by reducing the objective function. These objective functions are selected for reducing the time response features because of the error on time dependency ISTES. The role of fitness designated at the existing work is according to the ISTES for the simulation performance evaluation [25]–[27]. The ISTES fitness function is estimates from (9).

$$ISTES = \int_0^{\infty} [t^2 e(t)]^2 dt \quad (9)$$

The optimization problem can be formulated using the following rules,
Minimize (Objective function) Subjected to,

$$K_{pmin} < K_p < K_{pmax}$$

$$K_{imin} < K_i < K_{imax}$$

$$K_{dmin} < K_d < K_{dmax}$$

2.4. Optimization techniques

Meta-heuristic techniques are mainly divided into two main algorithm categories: single-based and population-based algorithm. Single-based algorithm is capable of generating a single optimal solution on every run. It is also called trajectory algorithm, and it is enhanced when a neighboring methodology is used. The population-based algorithm generates multiple solutions on every run and is further classified into five types: Swarm intelligence, human, physical, chemical, and evolutionary-based algorithms. In this evolutionary-based algorithm, the techniques use three main operations: Mutation, recombination, and selection. These techniques are inspired by nature's evolutionary phenomenon. For a swarm intelligent algorithm, the information is gathered on the basis of a collective behavior adopted by nature. Physical-based algorithm gathers information according to different theories obtained from the multiverse concept. Chemical-based algorithm uses chemical compounds and chemical rules for optimization while humans and their actions are associated with human-based algorithm. Population-based algorithms have a standard feature in common as per their nature, and the search processes in such algorithms are categorized into two phases: Exploitation and exploration [28]–[32]. The methodologies of optimization used in this study include grey wolf optimization (GWO) and SSA.

2.4.1. GWO

GWO algorithm is a recent technique introduced in 2014 by Mirjalili *et al.* [18]. There are four major types of simulations present in the grey wolves hierarchy. These types include Alpha (α) which present the best solution and is the leader, Beta (β) which is the second-best solution and has a role in assisting alpha in any decision process, Delta (δ) which is the third-best solution, and Omega (ω) is the rest of the population and also considered the worst-ranked [18]. The mathematical equations of GWO are given,

$$\vec{D} = |\vec{C} \cdot \vec{X}_p(t) - \vec{X}(t)| \quad (10)$$

$$\vec{X}(t+1) = \vec{X}_p(t) - \vec{A} \cdot \vec{D} \quad (11)$$

In this equation, t depicts the current iteration, whereas \vec{A} and \vec{C} denote the vector of coefficients. $X_p(t)$ is the position of vector in optimal solution reached up to this point and \vec{X} is GWO's position vector? \vec{A} and \vec{C} can be calculated by (12)-(13),

$$\vec{C} = 2 \cdot \vec{r} \quad (12)$$

$$\vec{A} = 2 \cdot \vec{a} \cdot \vec{r} - \vec{a} \quad (13)$$

In this equation, \vec{a} represents the variable that decreases linearly from 2 to 0 during a series of iteration. This equation represents the vector at random present in the interval from [0 1]. The algorithm then saves the top three best solutions are saved and searched on different search agents with the inclusion of omegas. The position in the best search agents is used to update their position. The beta, alpha, omega, and delta terms are defined by (14)-(16). The pseudocode and flowchart are described in Figure 3(a) and Figure 3(b), respectively.

$$\vec{D}_\alpha = |\vec{C}_1 \cdot \vec{X}_\alpha - \vec{X}|, \vec{D}_\beta = |\vec{C}_2 \cdot \vec{X}_\beta - \vec{X}|, \vec{D}_\delta = |\vec{C}_3 \cdot \vec{X}_\delta - \vec{X}| \quad (14)$$

$$\vec{X}_1 = \vec{X}_\alpha - \vec{A}_1 \cdot (\vec{D}_\alpha), \vec{X}_2 = \vec{X}_\beta - \vec{A}_2 \cdot (\vec{D}_\beta), \vec{X}_3 = \vec{X}_\delta - \vec{A}_3 \cdot (\vec{D}_\delta) \quad (15)$$

$$\vec{X}(t+1) = \frac{\vec{X}_1 + \vec{X}_2 + \vec{X}_3}{3} \quad (16)$$

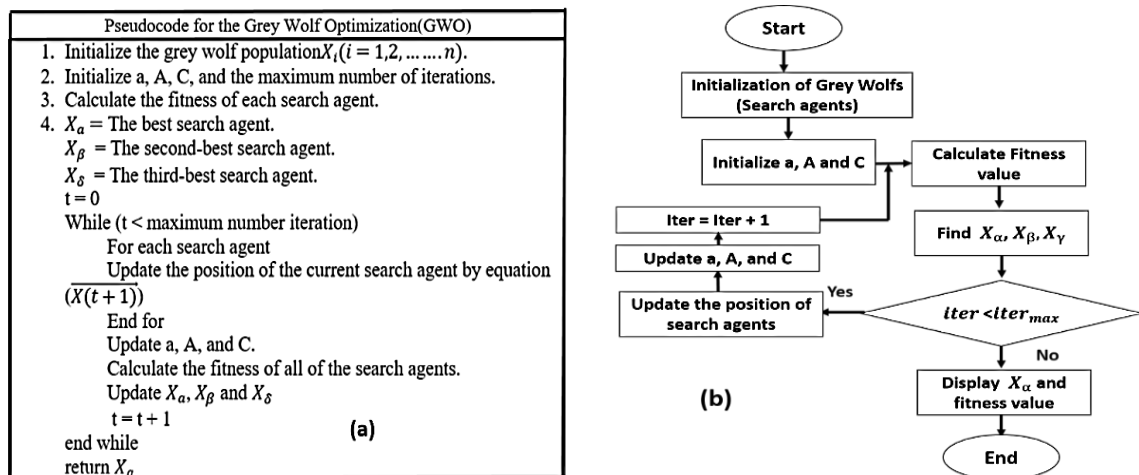


Figure 3. Solution procedure of GWO technique (a) Pseudocode and (b) Flowchart [18]

2.4.2. Sparrow search algorithm

As described, SSA is a technique of swarm intelligence optimization technique. The main idea behind this algorithm was inspired by closely observing the sparrow population's behavior and with the concept of foraging [33]. Depending on the behavioral characteristics, sparrows are classified into two groups; producers and scroungers. Producers are the ones who have a larger space to locate the sources of food and the other

group which search food according to the producers are called scroungers. The formula for SSA is determined by using (17)-(21).

Step 1: The matrix given is used to determine the position of sparrows.

$$X = \begin{bmatrix} X_{1,1} & \cdots & X_{1,d} \\ \vdots & \ddots & \vdots \\ X_{n,1} & \cdots & X_{n,d} \end{bmatrix} \quad (17)$$

In the equation presented, d represents the total dimension numbers, and n is the total sparrow number. In case of high energy levels in sparrows, they are called producers, and they are designated to find certain areas which have rich food supplies and to scavenge such zones to scroungers. Sparrow's value of cost is evaluated by (18),

$$F_x = \begin{bmatrix} f(X_{1,1} \cdots X_{1,d}) \\ \vdots \\ f(X_{n,1} \cdots X_{n,d}) \end{bmatrix} \quad (18)$$

Once sparrows locate the producers, alarming signals are produced for other sparrows depending upon the threshold criteria. Producers lead scroungers to a safe destination if the alarm's value exceeds the safety threshold's value. Producers which have the best cost value are most likely to find food as compared to the scroungers. In (19) is used to continuously update the position of producers.

$$X_{i,j}^{t+1} \begin{cases} X_{i,j}^t * \exp\left(-\frac{i}{\beta * iter_{max}}\right) & \text{if } R_2 < ST \\ X_{i,j}^t + Q * L & \text{if } R_2 \geq ST \end{cases} \quad (19)$$

In this equation, the producer's current position in the j th dimension present in an i th iteration is described by $X_{i,j}^t$ whereas the maximum number of iterations is denoted by $iter_{max}$. The value of the threshold is denoted by ST and falls in the range of $[0.5, 1]$, β denotes a random constant value ranging from $[0, 1]$, and the value R_2 lies within $[0, 1]$. So, according to this equation, it is considered that if the value of R_2 is lesser than the value of ST , there are zero predators, and producers can search for food sources globally. In other cases, R_2 is equal to or greater than ST . In (20) is used to update the position of scroungers. In this equation, A^+ is determined by $A^+ = A^T * (A * A^T)^{-1}$, X_p^{t+1} is the position value found by producer, and lastly, the value of the global worst population is represented by X_{worst} .

$$X_{i,j}^{t+1} \begin{cases} Q * \exp\left(\frac{X_{worst}^t - X_p^{t+1}}{i^2}\right) & \text{if } i > n/2 \\ X_p^{t+1} + |X_{i,j}^t - X_p^{t+1}| * A^+ * L & \text{Otherwise} \end{cases} \quad (20)$$

In (21) is used to determine the positions of producers. In this equation, X_{best}^t is the value of the current global optimal location, K is a random value, α is another random value which is normally distributed with a variance of 1 and mean value 0, and fw is the worst fitness value, f_i and f_g are the current individuals and current global best costs respectively. The pseudocode of SSA and the flowchart are present in Figure 4(a) and Figure 4(b), respectively.

$$X_{i,j}^{t+1} \begin{cases} X_{best}^t + \alpha * |X_{i,j}^t - X_{best}^{t+1}| * x & \text{if } f_i > f_g \\ X_{i,j}^t + K * \left(\frac{|X_{i,j}^t - X_{worst}^{t+1}|}{(f_i - f_{\omega}) + \varepsilon}\right) & \text{if } f_i = f_g \end{cases} \quad (21)$$

2.5. System architecture

The system architecture consists of seven components includes reservoir, coils, microparticles, pantograph robots, real-time controllers, microscope cameras, control algorithms, and power supply units. The microparticle's major components in 2D space would be presented by us as displayed in Figure 5. We utilized the controller of My Rio to arrive to a controller of real-time and for operation in real-time. We utilize four coils for controlling the 2D micro-particle position in the water. A COMSOL software was used for simulating the density of magnetic flux based on X and Y positions for particles coordination. The coil is made of isolated

copper wire with a 0.7mm dimension diam., the turns number is 1200. A robot of pantograph contains four links with two encoders for computing the 2 chief angles. The pantograph chief role is to permit the operator to controlling the trajectory of the micro-particle.

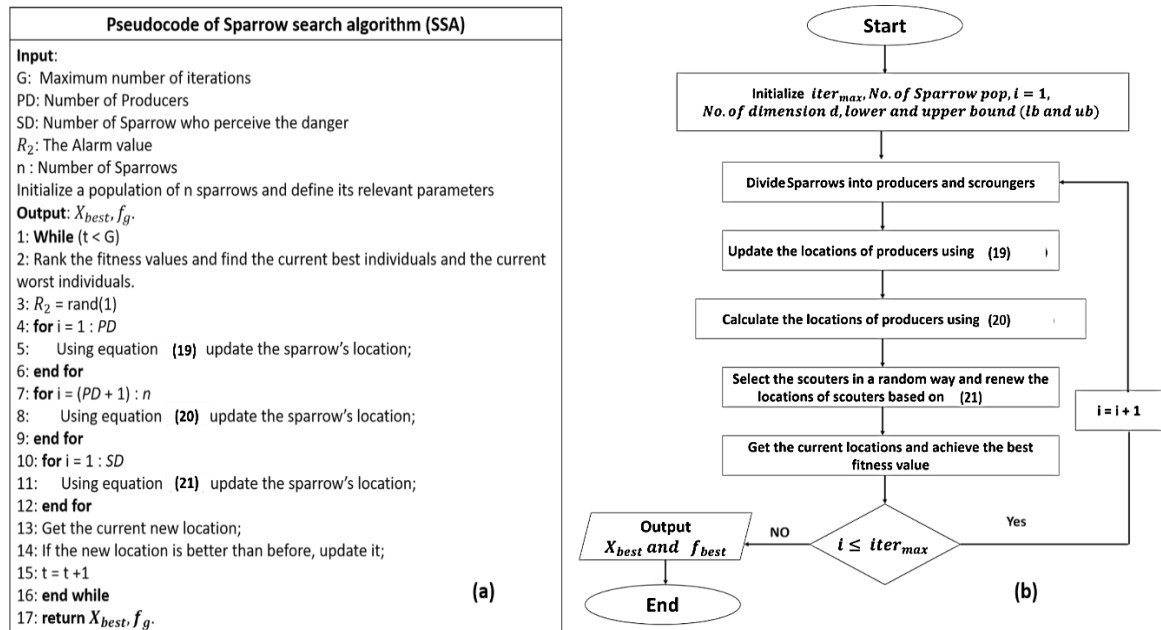


Figure 4. Solution procedure of SSA technique, (a) Pseudocode and (b) Flowchart [33]

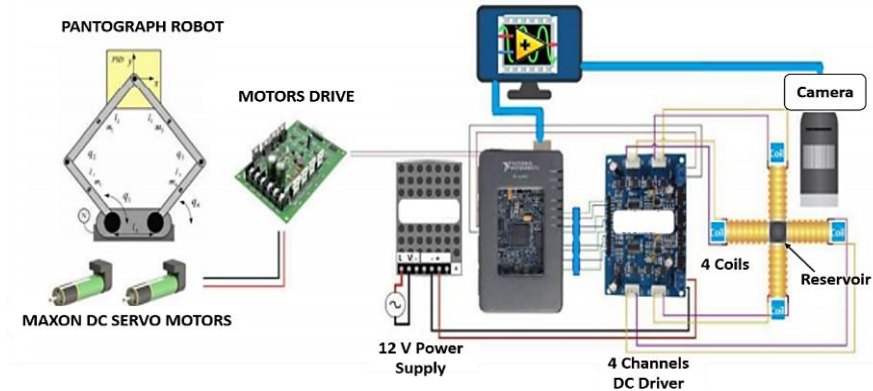


Figure 5. The complete system architecture to control micro-particle given in 2D space [3]

3. SIMULATION AND EXPERIMENTAL RESULTS

This section involves comprehensive details about the investigation of micro-robotics systems' performance by using multiple advanced control methods. Multiple tests are used to examine the execution of different control techniques and their performance. These techniques are examined at a constant position i.e. 1000 μm used as a reference command. A Simulink diagram displaying the different advanced control techniques in a micro-robotic system as shown in Figure 6. Regarding the maintenance and controlling of the micro-robotics system's position at 1000 μm , the parameters of GWO and SSA are presented in Table 1, and the proposed system parameters are listed in Table 2. Besides, Table 3 summarizes GWO and SSA output results based on different fitness functions in the time domain. Figure 7(a) and Figure 7(b) describe the behavior of a micro-robotics system by observing the reference of the position with the best fitness function (ISTES). The minor variance observed between the practical curves and the simulation is due to the card time acquisition delay, system uncertainty, and noise.

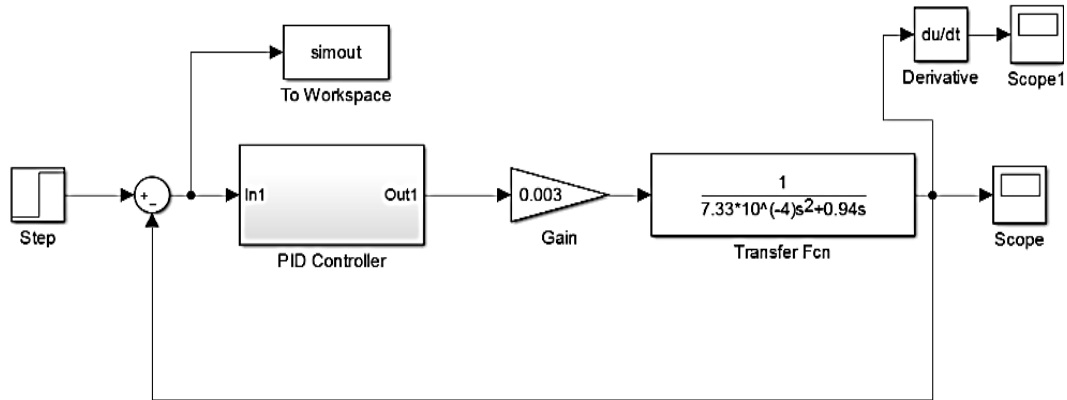


Figure 6. Simulink diagram of the micro-robotic system with different advanced control techniques

Table 1. GWO and SSA input parameter

GWO and SSA input parameters	
Parameters	Values
Number of variables (nVar)	3
Minimum value of variables (Kmin)	[0 0 0]
Maximum value of variables (Kmax)	[100 1 1]
Max number of iterations	25
Number of search agent	30

Table 2. The proposed system parameters

The proposed System Parameters		
Name	Values	Units
Radius (r)	50	μm
The density of Water (ρ)	998.2	kg m^{-3}
Dynamic Viscosity (ζ)	1	mPa s
Mass (m)	7.33×10^{-10}	Kg
Drag Coefficient (cd)	0.94×10^{-6}	N s m^{-2}

Table 3. GWO and SSA output results based on fitness functions (ISTES) in the time domain

(Ideal-PID) performance criteria	GWO						SSA					
	Control parameter			Settling error	Time response		Control parameter		Settling error	Time response		
	KP	KI	KD		t_r	t_s	KP	KI		KD	t_r	t_s
Simulation	90.7358	0.2566	0.0559	0	7.5607	13.1109	100	0.2672	0	0	6.8895	12.0744
Practical	90.7358	0.2566	0.0559	8	7.7083	13.1007	100	0.2672	0	4	7.0294	12.0655

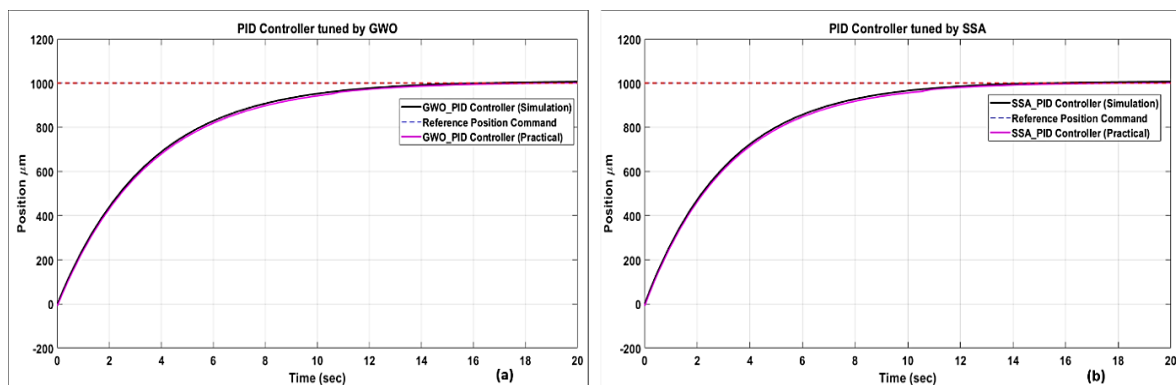


Figure 7. Position behavior of two optimization techniques based on PID control with fitness functions (ISTES): (a) GWO and (b) SSA

4. DISCUSSION

This section includes a thorough comparison between two methodologies of optimization which have been performed on different measurements in the time domain. The measurements include setting time (t_s), rising time (t_r), and settling error. The results of the previously recorded measurements on GWO and SSA are presented in Table 4.

Table 4. Comparison between GWO and SSA according to their time responses

No.	Control technique	t_r	t_s	Setting error(μm)
1	GWO Simulation	6.9574	12.0471	0
	Practical	7.7083	13.1007	8
2	SSA Simulation	6.8895	12.0744	0
	Practical	7.0294	12.1655	4

5. CONCLUSION

This paper includes the main optimization techniques which are used to tune the PID control in a micro-robotic system. It can be concluded that based on a set of different fitness functions to discover the best, the ISTES had the highest performance. A comparison between two main optimization techniques based on GWO and SSA was developed. It has been observed that SSA displays a very good performance when compared with GWO according to their rising and setting time and along with it several other measurements of performances were considered, due to which SSA is recommended to tune the PID parameters. SSA should be preferred over GWO because it enhances the efficiency of the parameter in the systems. It can be seen that the amount of error is decreased by 50% using SSA than other former experiments. For future practices, various optimization approaches such as whale optimization algorithm (WOA), hybrid PSO, Sine Cosine Algorithm (SCA), and flower pollination algorithm (FPA) will need further investigations.

ACKNOWLEDGEMENTS

I would like to thanks Dr. Mohamed Sallam for his support in the experimental setup.




REFERENCES

- [1] J. Keuning, "Image-based magnetic control of Microparticles," *University of Twente*, 2011, [Online]. Available: <http://essay.utwente.nl/70474/1/keuning2011msc.pdf>.
- [2] J. D. Keuning, J. de Vries, L. Abelmanny, and S. Misra, "Image-based magnetic control of paramagnetic microparticles in water," pp. 421–426, 2011, doi: 10.1109/iroso.2011.6095011.
- [3] R. Farag, I. Badawy, F. Magdy, Z. Mahmoud, and M. Sallam, "Real-Time Trajectory Control of Potential Drug Carrier Using Pantograph 'Experimental Study,'" *Advances in Intelligent Systems and Computing*, vol. 1261 AISC, pp. 305–313, 2021, doi: 10.1007/978-3-030-58669-0_28.
- [4] K. J. Astrom and T. Hagglund, "PID Controllers: theory, design, and tuning," *Instrument Society of America*, 1995.
- [5] M. Tamer, "PID Controller Implementation and Tuning," *InTech*, 2011.
- [6] T. Hagglund and K. J. Astrom, "Revisiting the Ziegler-Nichols tuning rules for PI control," *Asian Journal of Control*, vol. 4, no. 4, pp. 364–380, 2002, doi: 10.1111/j.1934-6093.2002.tb00076.x.
- [7] W. Tan, J. Liu, T. Chen, and H. J. Marquez, "Comparison of some well-known PID tuning formulas," *Computers and Chemical Engineering*, vol. 30, no. 9, pp. 1416–1423, 2006, doi: 10.1016/j.compchemeng.2006.04.001.
- [8] A. Visioli, "Research Trends for PID Controllers," *Acta Polytechnica*, vol. 52, no. 5, pp. 4–7, Jan. 2012, doi: 10.14311/1656.
- [9] D. Valério and J. S. da Costa, "Tuning of fractional PID controllers with Ziegler-Nichols-type rules," *Signal Processing*, vol. 86, no. 10, pp. 2771–2784, 2006, doi: 10.1016/j.sigpro.2006.02.020.
- [10] D. K. Maghade and B. M. Patre, "Pole placement by PID controllers to achieve time domain specifications for TITO systems," *Transactions of the Institute of Measurement and Control*, vol. 36, no. 4, pp. 506–522, 2014, doi: 10.1177/0142331213508803.
- [11] Q. V. Pham, S. Mirjalili, N. Kumar, M. Alazab, and W. J. Hwang, "Whale Optimization Algorithm with Applications to Resource Allocation in Wireless Networks," *IEEE Transactions on Vehicular Technology*, vol. 69, no. 4, pp. 4285–4297, 2020, doi: 10.1109/TVT.2020.2973294.
- [12] M. Bhuyan, D. C. Das, and A. K. Barik, "A Comparative analysis of DSM based autonomous hybrid microgrid using PSO and SCA," *Proceedings of 2019 IEEE Region 10 Symposium, TENSYP 2019*, pp. 765–770, 2019, doi: 10.1109/TENSYP46218.2019.8971155.
- [13] P. R. Chinda and R. Dalapati Rao, "A binary particle swarm optimization approach for power system security enhancement," *International Journal of Electrical and Computer Engineering (IJECE)*, vol. 12, no. 2, p. 1929, Apr. 2022, doi: 10.11591/ijece.v12i2.pp1929-1936.
- [14] M. Khalil Alsmadi et al., "Cuckoo algorithm with great deluge local-search for feature selection problems," *International Journal of Electrical and Computer Engineering (IJECE)*, vol. 12, no. 4, p. 4315, Aug. 2022, doi: 10.11591/ijece.v12i4.pp4315-4326.
- [15] A. C. Obula Reddy and K. Madhavi, "Manta ray optimized deep contextualized bi-directional long short-term memory based adaptive galactic swarm optimization for complex question answering," *International Journal of Electrical and Computer Engineering (IJECE)*, vol. 12, no. 4, p. 3994, Aug. 2022, doi: 10.11591/ijece.v12i4.pp3994-4006.
- [16] W. Aribowo, S. Supari, and B. Suprianto, "Optimization of PID parameters for controlling DC motor based on the aquila optimizer algorithm," *International Journal of Power Electronics and Drive Systems (IJPEDS)*, vol. 13, no. 1, p. 216, Mar. 2022, doi: 10.11591/ijped.v13i1.pp216-222.
- [17] M. Misaghi and M. Yaghoobi, "Improved invasive weed optimization algorithm (IWO) based on chaos theory for optimal design of PID controller," *Journal of Computational Design and Engineering*, vol. 6, no. 3, pp. 284–295, 2019, doi: 10.1016/j.jcde.2019.01.001.
- [18] S. Mirjalili, S. M. Mirjalili, and A. Lewis, "Grey wolf optimizer," *Advances in Engineering Software*, vol. 69, pp. 46–61, Mar. 2014, doi: 10.1016/j.advengsoft.2013.12.007.
- [19] S. M. Mirjalili, S. Z. Mirjalili, S. Saremi, and S. Mirjalili, "Sine cosine algorithm: Theory, literature review, and application in designing bend photonic crystal waveguides," *Studies in Computational Intelligence*, vol. 811, pp. 201–217, 2020, doi: 10.1007/978-3-030-12127-3_12.




- [20] R. Pradhan, S. K. Majhi, and B. B. Pati, "Design of PID controller for automatic voltage regulator system using Ant Lion Optimizer," *World Journal of Engineering*, vol. 15, no. 3, pp. 373–387, 2018, doi: 10.1108/WJE-05-2017-0102.
- [21] E. S. Ghith, F. A. Tolba, and S. A. Hammad, "Real-Time Implementation of Tuning PID Controller Based on Sine Cosine Algorithm for Micro-robotics System," pp. 801–811, 2022, doi: 10.1007/978-3-031-02447-4_82.
- [22] E. S. Ghith and F. Abdel Aziz Tolba, "Real-Time Implementation of Tuning PID Controller Based on Whale Optimization Algorithm for Micro-robotics System," *2022 14th International Conference on Computer and Automation Engineering, ICCAE 2022*, pp. 103–109, 2022, doi: 10.1109/ICCAE55086.2022.9762448.
- [23] E. S. Ghith and F. A. A. Tolba, "Design and Optimization of PID Controller using Various Algorithms for Micro-Robotics System," *Journal of Robotics and Control*, vol. 3, no. 3, pp. 244–256, 2022, doi: 10.18196/jrc.v3i3.14827.
- [24] K. G. Abdulhussein, N. M. Yasin, and I. J. Hasan, "Comparison of cascade P-PI controller tuning methods for PMDC motor based on intelligence techniques," *International Journal of Electrical & Computer Engineering*, vol. 12, no. 1, pp. 1–11, 2022, doi: 10.11591/ijece.v12i1.
- [25] E. S. G. M. M. Eissa, G. S. Virk, A. M. AbdelGhany, "Optimum Induction Motor Speed Control Technique using Genetic Algorithm," *American Journal of Intelligent Systems*, vol. 3, no. 1, pp. 1–12, 2013, doi: 10.5923/j.ajis.20130301.01.
- [26] E. S. G. M. M. Eissa, G. S. Virk, A. M. AbdelGhany, "Optimum Induction Motor Speed Control Technique using Particle Swarm Optimization," *International Journal of Energy Engineering*, vol. 3, no. 2, pp. 65–73, 2013, doi: 10.5923/J.IJEE.20130302.04.
- [27] M. Sallam, I. Saif, Z. Saeed, and M. Fanni, "Lyapunov-Based Control of a Teleoperation System in Presence of Time Delay," *Advances in Intelligent Systems and Computing*, vol. 1261 AISC, pp. 759–768, 2021, doi: 10.1007/978-3-030-58669-0_67.
- [28] D. Yousri, M. A. Elaziz, and S. Mirjalili, "Fractional-order calculus-based flower pollination algorithm with local search for global optimization and image segmentation," *Knowledge-Based Systems*, vol. 197, 2020, doi: 10.1016/j.knosys.2020.105889.
- [29] S. Li, H. Chen, M. Wang, A. A. Heidari, and S. Mirjalili, "Slime mould algorithm: A new method for stochastic optimization," *Future Generation Computer Systems*, vol. 111, pp. 300–323, 2020, doi: 10.1016/j.future.2020.03.055.
- [30] A. Yakout, W. Sabry, and H. M. Hasanien, "Enhancing rotor angle stability of power systems using marine predator algorithm based cascaded PID control," *Ain Shams Engineering Journal*, vol. 12, no. 2, pp. 1849–1857, 2021, doi: 10.1016/j.asej.2020.10.018.
- [31] M. A. Sobhy, A. Y. Abdelaziz, H. M. Hasanien, and M. Ezzat, "Marine predators algorithm for load frequency control of modern interconnected power systems including renewable energy sources and energy storage units," *Ain Shams Engineering Journal*, vol. 12, no. 4, pp. 3843–3857, 2021, doi: 10.1016/j.asej.2021.04.031.
- [32] A. Singh and S. Suhag, "Frequency regulation in an AC microgrid interconnected with thermal system employing multiverse-optimised fractional order-PID controller," *International Journal of Sustainable Energy*, vol. 39, no. 3, pp. 250–262, 2020, doi: 10.1080/14786451.2019.1684286.
- [33] J. Xue and B. Shen, "A novel swarm intelligence optimization approach: sparrow search algorithm," *Systems Science and Control Engineering*, vol. 8, no. 1, pp. 22–34, 2020, doi: 10.1080/21642583.2019.1708830.

BIOGRAPHIES OF AUTHORS



Ehab Saif Ghith    is born in Cairo, Egypt, on August 23, 1978. He is PhD Candidate. He received the B.Sc. degree in Design and Production Engineering in 2002 from the Faculty of Engineering at Ain shams University, Cairo, Egypt, M. Sc. in Systems Engineering and Engineering management, South Westphalia University of Applied Sciences, Germany 2013 and M.Sc. in System's Automation and Engineering Management, Helwan University, Egypt, 2013, Research topic: "Optimum induction Motor speed control technique using intelligent Methods". His research activity includes studying Artificial Intelligence, Electrical Machines, Automatic Control and Robotics. He can be contacted at email: Drehabghith1978@gmail.com



Farid Abdel Aziz Tolba    is born in Cairo, Egypt, on August 1, 1944. He is Professor at Mechatronics. He received the B.Sc. degree in Design and Production Engineering in 1969 from the Faculty of Engineering at Ain shams University, Cairo, Egypt, M. Sc. and PhD in Design and Production Engineering, 1972 and 1975 respectively, (Teaching Assistant on 1969-09-13-Assistant Lecturer on 1972-12-04-Lecturer on: 1975-10-27-Assistant Professor on 1980-12-01-Professor on 1986-02-03- Emeritus on 2004-08-01. His research activity includes studying Artificial Intelligence, Automatic Control and Robotics. He can be contacted at email: farid_tolba@eng.asu.edu.eg